HHS Public Access

Author manuscript

Toxicol Appl Pharmacol. Author manuscript; available in PMC 2016 August 15.

Published in final edited form as:

Toxicol Appl Pharmacol. 2015 August 15; 287(1): 86–92. doi:10.1016/j.taap.2015.05.011.

Safety evaluation of intravenously administered mono-thioated aptamer against E-selectin in mice

Shin-Ae Kang[1], **Bilegtsaikhan Tsolmon**[1], **Aman Mann**[2], **Wei Zheng**[1], **Lichao Zhao**[1], **Yan Daniel Zhao**[1], **David E. Volk**[2], **Ganesh L.-R. Lokesh**[2], **Lynsie Morris**[1], **Vineet Gupta**[1], **Wajeeha Razaq**[1], **Hallgeir Rui**[3], **Stephen K. Suh**[4], **David G. Gorenstein**[2], and **Takemi Tanaka**[1]

[1]Stephenson Cancer Center, University of Oklahoma Health Sciences Center, 975 NE, 10th, Oklahoma City, OK 73104

[2]Institute of Molecular Medicine and Department of NanoMedicine and Biomedical Engineering, University of Texas Health Science Center at Houston, 1825 Hermann Pressler, Houston, TX 77030

[3]Thomas Jefferson University, 1020 Locust St, Philadelphia, PA 19107

[4]John Theurer Cancer Center, Hackensack University Medical Center, Hackensack, NJ 07601

Abstract

The medical applications of aptamers have recently emerged. We developed an antagonistic thioaptamer (ESTA) against E-selectin. Previously, we showed that a single injection of ESTA at a dose of 100 μg inhibits breast cancer metastasis in mice through the functional blockade of E-selectin. In the present study, we evaluated the safety of different doses of intravenously administered ESTA in single-dose acute and repeat-dose subacute studies in ICR mice. Our data indicated that intravenous administration of up to 500 μg ESTA did not result in hematologic abnormality in either study. Additionally, intravenous injection of ESTA did not affect the levels of plasma cytokines (IL-1β, IL-2, IL-4, IL-5, IL-6, IL-10, GM-CSF, IFN-γ, and TNF-α) or complement split products (C3a and C5a) in either study. However, repeated injections of ESTA slightly increased plasma ALT and AST activities, in accordance with the appearance of small necrotic areas in the liver. In conclusion, our data demonstrated that intravenous administration of ESTA does not cause overt hematologic, organs, and immunologic responses under the experimental conditions.

Graphical abstract

Corresponding Author: Takemi Tanaka, Ph.D., Associate Professor, Stephenson Cancer Center at the University of Oklahoma Health Sciences Center, 975 NE 10th, BRC-W, Rm1415, Oklahoma City, OK 73104, Phone: Office (405)-271-8260, takemi-tanaka@ouhsc.edu.

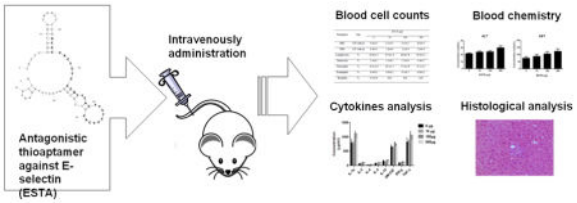

Keywords

mono-thioated aptamer; systemic toxicity; safety; E-selectin

1. Introduction

Aptamers, “chemical antibodies”, are structurally distinct RNA and DNA oligonucleotides that have been shown to mimic protein-binding molecules with high binding affinity (with Kd from pM to nM) and high selectivity (Keefe *et al.*, 2010). Aptamers are 1/10th the molecular weight of antibodies, yet provide complex tertiary structures with sufficient recognition surface area to exceed the effects of antibodies and small molecule inhibitors (Ellington and Szostak, 1990). A number of aptamers have been developed for various applications, including therapeutics, imaging, drug delivery, and diagnostics (Jayasena, 1999; Brody and Gold, 2000; Farokhzad *et al.*, 2006; Keefe *et al.*, 2010; Hong *et al.*, 2011). These chemical antibodies can target a wide range of molecules, from amino acids to live cells (Vianini *et al.*, 2001; Mann *et al.*, 2005; Shangguan *et al.*, 2006). Aptamers offer several advantages, including: 1) high binding affinity to their targets, 2) easy production and chemical modification, 3) low manufacturing costs, 4) long shelf-life, 5) CpG sequence-dependent immunogenicity, and 6) minimal batch-to-batch variation due to cell-free production. Therefore, aptamers are attractive candidates for medical applications. The systematic evolution of ligands by the exponential enrichment (SELEX) approach allows for the identification of aptamers that can bind to specific targets with high selectivity. Only a small number of aptamers are selected from the library by multiple iterations of selection (Ellington and Szostak, 1990; Tuerk and Gold, 1990). Thus far, several therapeutic aptamers, such as Pegaptanib (anti-VEGF;(Ruckman *et al.*, 1998), AptA and AptB (anti-Mucin 1; (Ferreira *et al.*, 2006), and AS1411 (anti-Nucleolin; (Bates *et al.*, 1999) have been successfully identified. Some of these have been used clinically or are currently undergoing clinical trials.

The major limitations of the clinical application of aptamers are their poor pharmaceutical properties and CpG sequence-dependent immunogenicity (Zhao *et al.*, 1999; Bouchard *et al.*, 2010). Structural modification of aptamers is essential to overcome these shortcomings (Soutschek *et al.*, 2004; Ulrich *et al.*, 2004; Burmeister *et al.*, 2005; Ng and Adamis, 2006; Keefe *et al.*, 2010). The sulfur substitution of the phosphate backbone or modification at the 2′ position of the ribose sugar to 2′-fluoro-ribose and 2′-O-methyl ribose has been shown to increase stability against nuclease, in turn improving the serum half-life (Thivi and Gorenstein, 2012). The conjugation of cholesterol or polyethylene glycol (PEG) to aptamers delays renal excretion (Soutschek *et al.*, 2004; Burmeister *et al.*, 2005). Pegaptanib (Macugen®), a 27- RNA aptamer, was modified with 2′-fluoro pyrimidines and 2′-O-methyl

purines and conjugated with 40 kDa PEG (Ng et al, 2006). Due to the unique sequence and backbone and structural modifications, the safety of each aptamer must be evaluated.

Previously, we developed ESTA, a thiophosphate-modified aptamer (thioaptamer) against E-selectin. ESTA is a 73-mer oligonucleotide that binds and antagonizes E-selectin (K_D= 47 nM; IC_{50} = 67–80 nM; (Mann *et al.*, 2010). We have demonstrated that ESTA inhibits the interaction between E-selectin and CD44, in turn inhibiting the adhesion of CD44+ breast cancer cells to inflamed endothelial cells. A single intravenous injection of 100 μg ESTA into mice *via* the tail vein prevented the development of breast cancer lung metastasis in a forced lung metastasis model (Kang *et al.*, 2015). In the present study, we evaluated the safety of intravenously administered ESTA in mice, using both single-dose acute and repeat-dose subacute studies to explore the possible applications of ESTA to the prevention of breast cancer lung metastasis.

2. Materials and methods

2.1. Aptamer

ESTA, the thioaptamer against E-selectin, is a 73-mer thiophosphate-modified oligodeoxynucleotide aptamer with sequence d(5′-CGCTCGGATCGATAAGCTTCGATCCCACTCTCCCGTTCACTTCTCCTCACGTCACGGATCCTCTAGAGCACTG -3′), in which one of the non-bridging phosphoryl oxygens in the oligonucleotide phosphate backbone is substituted with sulfur on the 5′-side of all dA bases after dA22.

2.2. Animals and study design

Six-week-old ICR mice were purchased from Taconic Farms (Germantown, NY, USA). The mice (n=7–9; 4–5 male, 4–5 female) were randomly assigned into four groups. The overall average weight of each group was 31.5g (35.8 g in males, 27.5 g in females). All animal housing and experimental procedures were performed in accordance with the institutional guidelines of the University of Oklahoma. In the single-dose acute study, mice received a single intravenous injection of one of three dose levels of ESTA (10 μg, 100 μg, and 500 μg in 100 μl saline per mouse), or 100 μl of saline *via* the tail vein. Four hours after the injection, the mice were anesthetized to collect whole blood by cardiac puncture. The whole blood was used for hematological evaluations, and the plasma was isolated for blood chemistry and cytokine analyses. In the repeat-dose subacute study, mice received a single intravenous injection of one of three dose levels of ESTA (10 μg, 100 μg, and 500 μg in 100 μl saline per mouse) or 100 μl of saline *via* the tail vein twice a week for 4 weeks. Two days after the last injection, whole blood was collected by cardiac puncture and plasma were prepared for hematologic evaluation and blood chemistry and cytokine analyses, respectively. The major organs (liver, spleen, kidneys, lungs, and heart) were harvested for histological evaluation in both single-dose acute and repeat-dose subacute studies.

2.3. Blood cell counts

White blood cell (WBC) and red blood cell (RBC) counts were measured using a Countess Automated Cell Counter (Life Technologies, Carlsbad, CA, USA). The peripheral blood

smear slides were stained using Camco Stain Pac (Cambridge Diagnostics Products, Fort Lauderdale, FL, USA) for blood differential staining. Differential WBC counts were then performed under 40× magnification with a Leica DM2500 microscope (Leica, Buffalo Grove, IL, USA). The number of lymphocytes, monocytes, neutrophils, eosinophils, and basophils were counted from a minimum of one hundred WBCs using standard morphologic criteria.

2.4. Blood chemistry

Hepatic and renal function were evaluated using commercial assay kits for plasma alanine transaminase (BioVision, Milpitas, CA, USA), aspartate transaminase (BIOO Scientific, Austin, TX, USA), and urea (BioAssay Systems, Hayward, CA, USA). Complementary activation was analyzed by measuring C3a and C5a concentrations in plasma using ELISA kits obtained from GenWay Biotech (San Diego, CA, USA) and RayBioTech (Norcross, GA, USA), respectively, according to the manufacturer's instructions.

2.5. Cytokines analysis

Cytokine levels (IL-1β, IL-2, IL-4, IL-5, IL-10, GM-CSF, IFN-γ, and TNF-α) were measured using the Bio-Plex Pro™ Mouse Cytokine 8-plex assay kit and Bio-Plex 200 system (Bio-Rad Laboratories, Hercules, CA, USA), according to the manufacturer's instructions. IL-6 was measured using an ELISA kit from RayBioTech (Norcross, GA, USA), according to the manufacturer's instructions.

2.6. Histologic analysis

Histologic analysis was performed on formalin-fixed, paraffin-embedded (FFPE) tissue. The tissues were fixed in 10% neutral-buffered formalin overnight and were dehydrated, cleared, embedded in paraffin, cut into 4-μm-thick sections, and stained with hematoxylin and eosin (H&E) and PAS to assess histology. H&E and PAS staining of tissue sections were performed by the Tissue Pathology Core at the University of Oklahoma Health Sciences Center, using a Leica STS5020 Multistainer (Leica, Buffalo Grove, IL, USA). Tissue sections were examined using an Olympus light microscope (BX41; Olympus America, Center Valley, PA, USA), and the images were converted to digital slides using an Aperio scanner (AT2; Leica), and analyzed with a computer-assisted image analysis system (Aperio ScanScope™; Leica).

2.7. Statistical analysis

Due to the widespread dose range (0 μg, 10 μg, 100 μg, 500 μg), a log dose variable [l dose=log (dose+2.718)] was computed and subsequently used as an alternative to dose in the statistical analyses. A constant 2.718 was added to dose in the log transformation to account for the original 0 μg dose group. The relationship between testing parameters and one dose was first examined using a scatter plot with local regression (LOESS) curve fitting and subsequent diagnostic residual plots. If a linear relationship existed, then the simple linear regression was fitted. Otherwise, the one-way ANOVA method with Dunnett's adjustment was used to compare the values of testing parameters between each dose and the control dose. All p values less than 0.05 were considered statistically significant. SAS 9.2 was used

in the statistical analysis. The area of necrotic foci was compared between saline and ESTA-injected groups using the two-sample t-test with unequal variances. The difference in number of intralobular necrotic foci and the proportion of mice with at least one positive intralobular necrotic foci between saline and ESTA (500 μg) was analyzed using the Wilcoxon Rank sum test and the Fisher's exact test, respectively.

3. Results

3.1. The effect of ESTA on blood cell counts

Total red blood cells (RBC), total white blood cells (WBC), and absolute differential WBC were counted following a single-dose acute or repeat-dose subacute intravenous administration of one of three dose of levels of ESTA (10 μg, 100 μg, and 500 μg) in ICR mice. The administration of ESTA did not change total RBC and WBC counts in either the single-dose acute (Table 1) or repeat-dose subacute study (Table 2). Total RBC and WBC counts in all experimental groups remained in the normal reference range (Hedrich, 2012). In addition, there was no statistically significant difference in WBC differential between saline-injected control group and ESTA-injected groups at any dose used in this study (Table 1 and Table 2). These data show that neither single nor repeated intravenous injections of ESTA caused significant changes in blood cell counts.

3.2. The effect of ESTA on renal and hepatic functions

To examine the effect of ESTA on hepatic and renal functions, we measured alanine transaminase (ALT) and aspartate transaminase (AST) activities in the plasma collected from the mice that had been intravenously injected with ESTA twice weekly for one month. At the 500 μg dose level, we detected significant increases in both ALT (Fig. 1A, 29.9 ±2.9 vs. control 21.6 ± 0.8 Units/L, p=0.006) and AST (Fig. 1B, 124.1±17.2 vs. control 75.2 ± 10.3 Units/L, p=0.046). However, for the 10 and 100 μg doses, no statistically significant changes in ALT or AST levels were found, compared with saline-injected controls. The ALT and AST elevations were dose-related (p=0.003 for ALT and p=0.01 for AST, linear regression model). In contrast, repeated doses of ESTA did not cause a significant change in the BUN levels in any experimental dose group, and no dose-related response was noted. This indicated that ESTA did not cause significant kidney toxicity (Fig. 1C). In accordance with the dose-related ALT and AST elevations, small focal hepatocellular foci was noted histologically in tissues from mice that were administered 500 μg ESTA twice a week for 4 weeks (Fig. 2A). The PAS staining confirmed that the focal hepatocellular necrotic foci were necrotic foci admixed with a few lymphocytes, although this change was minor pathologically, as these foci were not intensely or diffusely distributed throughout the liver parenchyma (Fig. 2A). Statistical analysis supported the pathologic evaluation of no significant differences in the proportion of mice with at least one positive intra-lobular necrotic foci (33.3% vs. 75.0%, p=0.153), or in the area of necrotic foci (18603 vs. 2825, p=0.445; Fig. 2B), in the saline-injected group and the ESTA-injected group, respectively. However, fewer intra-lobular necrotic foci were observed in the saline-injected group than in the ESTA-injected group (0 vs. 1.5, p=.036). In addition, no sign of hepatitis, fibrosis, steatosis, or pathogenic organisms was observed following ESTA administration. No

obvious toxicity was detected in other organs, including lungs, spleens, and hearts, at least on a histopathologic level (Supplementary Fig. 1).

3.3. The effect of ESTA on complement activation and the levels of cytokines

The effect of ESTA on complement activation (C3a and C5a) was assessed following single and repeated administration of various doses of ESTA. No ESTA-related differences were observed in C3a activation when drug-injected animals were compared with controls (Fig. 3A and 3B). Similarly, there were no significant differences in C5a following single or repeated intravenous injection of ESTA compared with the control group (Fig. 3C and 3D). These results suggested that doses of up to 500 μg of ESTA do not activate the C3a and C5a complement pathways. To determine whether single or repeated administration of ESTA alters plasma cytokine levels, we evaluated the plasma levels of eight different cytokines: IL-1β, IL-2, IL-4, IL-5, IL-10, GM-CSF, IFN-γ, and TNF-α (Fig. 4A and 4B). In the single-dose acute study, most cytokines, except IL-10, trended toward a slight increase in ESTA-injected groups (100 μg and 500 μg) when compared with saline-injected control groups, but these trends were not statistically significant ($p > 0.05$; Fig 4A). In the repeat-dose subacute study, there were no significant changes in any tested cytokine levels (Fig 4B). The baseline levels of all tested cytokines were consistently higher in the single-dose acute study control group than in the repeat-dose subacute study control group. The difference in baseline levels may be due to different intervals between the last intravenous administration of ESTA and blood collection (4 h in single-dose acute vs. 48 h in repeat-dose subacute). In addition to the above cytokines, the plasma concentration of IL-6 was measured to evaluate the potential effects of CpG present within the ESTA sequence. Previous studies reported that an unmethylated CpG motif causes the activation of innate immune response and induces the secretion of cytokines, including IL-6 and interferon (Klinman *et al.*, 1996; Krieg, 1999; Krieg, 2006). IL-6 levels were unaffected by the administration of any dose of ESTA in both the single-dose acute and repeat-dose subacute studies (Fig. 4C and 4D). Together, these results indicated that intravenous injection of ESTA at doses up to 500 μg did not cause acute or subacute immunogenicity in mice.

4. Discussion

We previously reported that an antagonistic thioaptamer against E-selectin (ESTA) specifically target E-selectin (Mann *et al.*, 2010) and that a single bolus intravenous injection of ESTA at a dose of 100 μg is effective to prevent the development of metastasis in mouse models of forced metastasis (Kang *et al.*, 2015). Our previous studies also indicated that twice weekly intravenous injections of 100 μg of ESTA were necessary to achieve therapeutic effects in a model of spontaneous metastasis, but a single weekly injection of the same dose of ESTA did not provide therapeutic benefit (data not shown). Based on these studies, we performed dose-ranging single-dose acute and repeat-dose subacute safety studies.

Earlier studies show that intravenously administered oligonucleotides are rapidly distributed from the circulation to the parenchyma in various organs, and then accumulate primarily in the liver, kidneys, and spleen (Geary *et al.*, 2003). Administration of oligonucleotides at

doses of 100 mg/kg *via* intraperitoneal injection or 50 mg/kg *via* intravenous injection has been reported to cause reversible renal and hepatic abnormalities in mice after 4–13 weeks of dose-free recovery (Sarmiento *et al.*, 1994; Henry *et al.*, 1997b; Bouchard *et al.*, 2010). These abnormalities are characterized by mononuclear infiltration, hypertrophy of Kupffer cells in the liver, and basophilic granules within the cytoplasm of tubular epithelial cells in kidneys (Henry *et al.*, 1997a; Henry *et al.*, 1999; Bouchard *et al.*, 2010). Our data show that ESTA did not cause changes in BUN level, kidney histomorphology, and body weight at doses of up to 500 μg. There was no definitive evidence of sinusoidal dilation, Kupffer cell hypertrophy, or perivascular inflammatory infiltrate in the liver after comparing control and ESTA-injected groups. However, we found that the intravenous injection of 500 μg of ESTA caused slight increases in ALT and AST levels (1.4-fold and 1.7-fold increases compared with the control group, respectively). The increased liver enzymes were associated with minor histological abnormalities, which included scattered intra-lobular necrotic foci admixed with infiltrated lymphocytes. Overall, on the basis of the alterations of liver enzyme activities along with pathologic evaluation, hepatic tissue abnormalities were minor, and this change was not severe enough to achieve the maximum tolerated dose of ESTA. The effective therapeutic dose of ESTA (100 μg) falls significantly below the maximum tolerated dose (Kang *et al.*, 2015), and the maximum tolerated dose of ESTA need to be further determined in future studies.

Previous studies reported that aptamers also cause a sequence-dependent adverse effect. It is reported that the unmethylated CpG motif of DNA is recognized by TLR9, which in turn stimulates the production of cytokines, including type I interferon and interleukin-6 (Klinman *et al.*, 1996; Krieg, 1999; Krieg, 2006). The CpG motif consists of an unmethylated CpG dinucleotide flanked by particular base contexts, such as two 5′-purines and two 3′-pyrimidines (Krieg *et al.*, 1995). For example, the CpG motif with the "TCAACGTT" sequence was shown to induce B-cell activation, whereas a similar sequence, "TCATCGAT", was non-immunogenic. ESTA contains seven CpG motifs. However, none of the CpG motifs are flanked by either two 5′-purines or two 3′-pyrimidines (ESTA sequence: 5′-CGCTCGGATCGATAAGCTTCGATCCCACTCTCCCGTTCACTTCTCCTCACGTCACG GATCCTCTAGAGCACTG -3′). As a result, intravenous administration of ESTA did not cause significant changes in plasma IL-6, a direct downstream target of TRL9, in either single-dose acute or repeat-dose subacute studies, further suggesting the safe application of ESTA.

E-selectin (CD62E, ELAM-1, or LECAM-2) is inducibly expressed on the surfaces of endothelial cells in response to inflammatory cytokines (Bevilacqua, 1993), and mediates rolling and adhesion of circulating leukocytes and cancer cells through the interaction with its counter receptor ligands, sialyl Lewis^{x} (sLe^{x}) and sialyl Lewis^{A} (sLe^{A}; (Phillips *et al.*, 1990; Picker *et al.*, 1991; Shimizu *et al.*, 1991; Zetter, 1993; Nguyen *et al.*, 2009). Consequently, elevated E-selectin expression on the vessel wall is observed in many types of inflammatory disease, including cancer, diabetes, coronary artery disease, and rheumatoid arthritis (Grober *et al.*, 1993; Tozeren *et al.*, 1995; Dong *et al.*, 1998; Meigs *et al.*, 2004; Barthel *et al.*, 2007). It is well documented that chronic inflammation leads to a pathologic tissue infiltration of immune cells (Luster *et al.*, 2005), and the control of chronic

inflammation remains a challenge due to the lack of suitable molecular target. We have shown that a single bolus intravenous injection of ESTA at a dose of 100 μg has the ability to inhibit hematogenous metastasis *in vivo via* the blockade of interaction between E-selectin and cancer cells in the circulation (Kang *et al.*, 2015). The possible clinical applications of such therapeutic aptamers are not limited to cancer, and may be applicable to the control of chronic inflammatory diseases for the control of pathologic inflammation via the blockade of E-selectin.

Clinical applications of aptamers have recently emerged and are broadly accepted as a new class of high-affinity ligand. Similar to monoclonal antibodies, aptamers function as therapeutics (Brody and Gold, 2000; Keefe *et al.*, 2010) and as targeting moieties in a delivery system (Farokhzad *et al.*, 2006; Huang *et al.*, 2009). Aptamer-conjugated drugs or nanoparticles have been developed for the selective delivery of therapeutic payload to disease sites, while sparing systemic toxicity of drug and accumulation of particles in the reticuloendothelial system (RES), e.g., the liver, kidney, spleen, and lymph nodes (Sarmiento *et al.*, 1994; Henry *et al.*, 1997b). The biodistribution and pharmacokinetic parameters of aptamer-conjugated delivery carrier or drug are expected to be different from aptamer alone or delivery carrier alone. Thus, the safety of these delivery system will need to be evaluated individually to assess potential bystander effects. All therapeutic aptamers have the backbone modification and PEGylation to improve the resistance against nuclease and pharmacokinetic parameters. ESTA's DNA backbone is mono-thioated to provide nuclease resistance. As a result, ESTA is stable in the serum for up to 16 hours *in vitro* (Supplementary Figure 2). However, the serum half-life of ESTA *in vivo* is as short as 3.09 min. While ESTA binds to E-selectin on the inflamed vessels and remains bound to the lung, liver, and kidney for at least 6 hours after the injection, further modification, such as PEGylation, to improve its serum stability is essential for realistic translation to clinical applications. In conclusion, we demonstrated that single-dose acute and repeat-dose subacute intravenous administration of ESTA are well tolerated at doses of up to 500 μg in male and female ICR mice.

Supplementary Material

Refer to Web version on PubMed Central for supplementary material.

Acknowledgments

This work was supported by the Department of Defense (W81XWH-11-1-0238), the National Institutes of Health (1R01CA160271-01A1), the American Cancer Society (IRG-08-060-04), and the Pennsylvania Breast Cancer Coalition to T. Tanaka, and U54CA151668 to D. Gorenstein. We thank the Pathology Core at the University of Oklahoma. David Gorenstein is a founder of AM Biotechnologies, which has licensed thioaptamer selection technologies.

References

Barthel SR, Gavino JD, Descheny L, Dimitroff CJ. Targeting selectins and selectin ligands in inflammation and cancer. Expert opinion on therapeutic targets. 2007; 11:1473–1491. [PubMed: 18028011]

Bates PJ, Kahlon JB, Thomas SD, Trent JO, Miller DM. Antiproliferative activity of G-rich oligonucleotides correlates with protein binding. The Journal of biological chemistry. 1999; 274:26369–26377. [PubMed: 10473594]

Bevilacqua MP. Endothelial-leukocyte adhesion molecules. Annual review of immunology. 1993; 11:767–804.

Bouchard PR, Hutabarat RM, Thompson KM. Discovery and development of therapeutic aptamers. Annual review of pharmacology and toxicology. 2010; 50:237–257.

Brody EN, Gold L. Aptamers as therapeutic and diagnostic agents. Journal of biotechnology. 2000; 74:5–13. [PubMed: 10943568]

Burmeister PE, Lewis SD, Silva RF, Preiss JR, Horwitz LR, Pendergrast PS, McCauley TG, Kurz JC, Epstein DM, Wilson C, Keefe AD. Direct in vitro selection of a 2′-O-methyl aptamer to VEGF. Chemistry & biology. 2005; 12:25–33. [PubMed: 15664512]

Dong ZM, Chapman SM, Brown AA, Frenette PS, Hynes RO, Wagner DD. The combined role of P- and E-selectins in atherosclerosis. The Journal of clinical investigation. 1998; 102:145–152. [PubMed: 9649568]

Ellington AD, Szostak JW. In vitro selection of RNA molecules that bind specific ligands. Nature. 1990; 346:818–822. [PubMed: 1697402]

Farokhzad OC, Cheng J, Teply BA, Sherifi I, Jon S, Kantoff PW, Richie JP, Langer R. Targeted nanoparticle-aptamer bioconjugates for cancer chemotherapy in vivo. Proceedings of the National Academy of Sciences of the United States of America. 2006; 103:6315–6320. [PubMed: 16606824]

Ferreira CS, Matthews CS, Missailidis S. DNA aptamers that bind to MUC1 tumour marker: design and characterization of MUC1-binding single-stranded DNA aptamers. Tumour biology : the journal of the International Society for Oncodevelopmental Biology and Medicine. 2006; 27:289–301. [PubMed: 17033199]

Geary RS, Yu RZ, Watanabe T, Henry SP, Hardee GE, Chappell A, Matson J, Sasmor H, Cummins L, Levin AA. Pharmacokinetics of a tumor necrosis factor-alpha phosphorothioate 2′-O-(2-methoxyethyl) modified antisense oligonucleotide: comparison across species. Drug metabolism and disposition: the biological fate of chemicals. 2003; 31:1419–1428. [PubMed: 14570775]

Grober JS, Bowen BL, Ebling H, Athey B, Thompson CB, Fox DA, Stoolman LM. Monocyte-endothelial adhesion in chronic rheumatoid arthritis. In situ detection of selectin and integrin-dependent interactions. The Journal of clinical investigation. 1993; 91:2609–2619. [PubMed: 7685772]

Hedrich, HJ. The Laboratory Mouse. Academic Press; 2012.

Henry SP, Taylor J, Midgley L, Levin AA, Kornbrust DJ. Evaluation of the toxicity of ISIS 2302, a phosphorothioate oligonucleotide, in a 4-week study in CD-1 mice. Antisense & nucleic acid drug development. 1997a; 7:473–481. [PubMed: 9361906]

Henry SP, Templin MV, Gillett N, Rojko J, Levin AA. Correlation of toxicity and pharmacokinetic properties of a phosphorothioate oligonucleotide designed to inhibit ICAM-1. Toxicologic pathology. 1999; 27:95–100. [PubMed: 10367680]

Henry SP, Zuckerman JE, Rojko J, Hall WC, Harman RJ, Kitchen D, Crooke ST. Toxicological properties of several novel oligonucleotide analogs in mice. Anti-cancer drug design. 1997b; 12:1–14. [PubMed: 9051110]

Hong H, Goel S, Zhang Y, Cai W. Molecular imaging with nucleic acid aptamers. Current medicinal chemistry. 2011; 18:4195–4205. [PubMed: 21838686]

Huang YF, Shangguan D, Liu H, Phillips JA, Zhang X, Chen Y, Tan W. Molecular assembly of an aptamer-drug conjugate for targeted drug delivery to tumor cells. Chembiochem : a European journal of chemical biology. 2009; 10:862–868. [PubMed: 19253922]

Jayasena SD. Aptamers: an emerging class of molecules that rival antibodies in diagnostics. Clinical chemistry. 1999; 45:1628–1650. [PubMed: 10471678]

Kang SA, Hasan N, Mann AP, Zheng W, Zhao L, Morris L, Zhu W, Zhao D, Suh KS, Dooley WC, Volk D, Gorenstein DG, Cristofanilli M, Rui H, Tanaka T. Blocking the Adhesion Cascade at the Pre-metastatic Niche for Prevention of Breast Cancer Metastasis. Molecular therapy : the journal of the American Society of Gene Therapy. 2015

Keefe AD, Pai S, Ellington A. Aptamers as therapeutics. Nature reviews Drug discovery. 2010; 9:537–550.

Klinman DM, Yi AK, Beaucage SL, Conover J, Krieg AM. CpG motifs present in bacteria DNA rapidly induce lymphocytes to secrete interleukin 6, interleukin 12, and interferon gamma. Proceedings of the National Academy of Sciences of the United States of America. 1996; 93:2879–2883. [PubMed: 8610135]

Krieg AM. Mechanisms and applications of immune stimulatory CpG oligodeoxynucleotides. Biochimica et biophysica acta. 1999; 1489:107–116. [PubMed: 10807001]

Krieg AM. Therapeutic potential of Toll-like receptor 9 activation. Nature reviews Drug discovery. 2006; 5:471–484. [PubMed: 16763660]

Krieg AM, Yi AK, Matson S, Waldschmidt TJ, Bishop GA, Teasdale R, Koretzky GA, Klinman DM. CpG motifs in bacterial DNA trigger direct B-cell activation. Nature. 1995; 374:546–549. [PubMed: 7700380]

Luster AD, Alon R, von Andrian UH. Immune cell migration in inflammation: present and future therapeutic targets. Nature immunology. 2005; 6:1182–1190. [PubMed: 16369557]

Mann AP, Somasunderam A, Nieves-Alicea R, Li X, Hu A, Sood AK, Ferrari M, Gorenstein DG, Tanaka T. Identification of thioaptamer ligand against E-selectin: potential application for inflamed vasculature targeting. PloS one. 2010:5.

Mann D, Reinemann C, Stoltenburg R, Strehlitz B. In vitro selection of DNA aptamers binding ethanolamine. Biochemical and biophysical research communications. 2005; 338:1928–1934. [PubMed: 16289104]

Meigs JB, Hu FB, Rifai N, Manson JE. Biomarkers of endothelial dysfunction and risk of type 2 diabetes mellitus. Jama. 2004; 291:1978–1986. [PubMed: 15113816]

Ng EW, Adamis AP. Anti-VEGF aptamer (pegaptanib) therapy for ocular vascular diseases. Annals of the New York Academy of Sciences. 2006; 1082:151–171. [PubMed: 17145936]

Nguyen DX, Bos PD, Massague J. Metastasis: from dissemination to organ-specific colonization. Nature reviews Cancer. 2009; 9:274–284. [PubMed: 19308067]

Phillips ML, Nudelman E, Gaeta FC, Perez M, Singhal AK, Hakomori S, Paulson JC. ELAM-1 mediates cell adhesion by recognition of a carbohydrate ligand, sialyl-Lex. Science. 1990; 250:1130–1132. [PubMed: 1701274]

Picker LJ, Kishimoto TK, Smith CW, Warnock RA, Butcher EC. ELAM-1 is an adhesion molecule for skin-homing T cells. Nature. 1991; 349:796–799. [PubMed: 1705666]

Ruckman J, Green LS, Beeson J, Waugh S, Gillette WL, Henninger DD, Claesson-Welsh L, Janjic N. 2′-Fluoropyrimidine RNA-based aptamers to the 165-amino acid form of vascular endothelial growth factor (VEGF165). Inhibition of receptor binding and VEGF-induced vascular permeability through interactions requiring the exon 7-encoded domain. The Journal of biological chemistry. 1998; 273:20556–20567. [PubMed: 9685413]

Sarmiento UM, Perez JR, Becker JM, Narayanan R. In vivo toxicological effects of rel A antisense phosphorothioates in CD-1 mice. Antisense research and development. 1994; 4:99–107. [PubMed: 7950306]

Shangguan D, Li Y, Tang Z, Cao ZC, Chen HW, Mallikaratchy P, Sefah K, Yang CJ, Tan W. Aptamers evolved from live cells as effective molecular probes for cancer study. Proceedings of the National Academy of Sciences of the United States of America. 2006; 103:11838–11843. [PubMed: 16873550]

Shimizu Y, Shaw S, Graber N, Gopal TV, Horgan KJ, Van Seventer GA, Newman W. Activation-independent binding of human memory T cells to adhesion molecule ELAM-1. Nature. 1991; 349:799–802. [PubMed: 1705667]

Soutschek J, Akinc A, Bramlage B, Charisse K, Constien R, Donoghue M, Elbashir S, Geick A, Hadwiger P, Harborth J, John M, Kesavan V, Lavine G, Pandey RK, Racie T, Rajeev KG, Rohl I, Toudjarska I, Wang G, Wuschko S, Bumcrot D, Koteliansky V, Limmer S, Manoharan M, Vornlocher HP. Therapeutic silencing of an endogenous gene by systemic administration of modified siRNAs. Nature. 2004; 432:173–178. [PubMed: 15538359]

Thiviyanathan V, Gorenstein DG. Aptamers and the next generation of diagnostic reagents. Proteomics Clinical applications. 2012; 6:563–573. [PubMed: 23090891]

Tozeren A, Kleinman HK, Grant DS, Morales D, Mercurio AM, Byers SW. E-selectin-mediated dynamic interactions of breast- and colon-cancer cells with endothelial-cell monolayers. International journal of cancer Journal international du cancer. 1995; 60:426–431. [PubMed: 7530236]

Tuerk C, Gold L. Systematic evolution of ligands by exponential enrichment: RNA ligands to bacteriophage T4 DNA polymerase. Science. 1990; 249:505–510. [PubMed: 2200121]

Ulrich H, Martins AH, Pesquero JB. RNA and DNA aptamers in cytomics analysis. Cytometry Part A : the journal of the International Society for Analytical Cytology. 2004; 59:220–231. [PubMed: 15170601]

Vianini E, Palumbo M, Gatto B. In vitro selection of DNA aptamers that bind L-tyrosinamide. Bioorganic & medicinal chemistry. 2001; 9:2543–2548. [PubMed: 11557341]

Zetter BR. Adhesion molecules in tumor metastasis. Seminars in cancer biology. 1993; 4:219–229. [PubMed: 8400144]

Zhao Q, Yu D, Agrawal S. Site of chemical modifications in CpG containing phosphorothioate oligodeoxynucleotide modulates its immunostimulatory activity. Bioorganic & medicinal chemistry letters. 1999; 9:3453–3458. [PubMed: 10617090]

Highlights

- Intravenous administration of ESTA was well tolerated.
- ESTA up to 500 μg does not cause hematologic, organs, and immunologic responses.
- ESTA-mediated hepatic abnormality was considered minor.

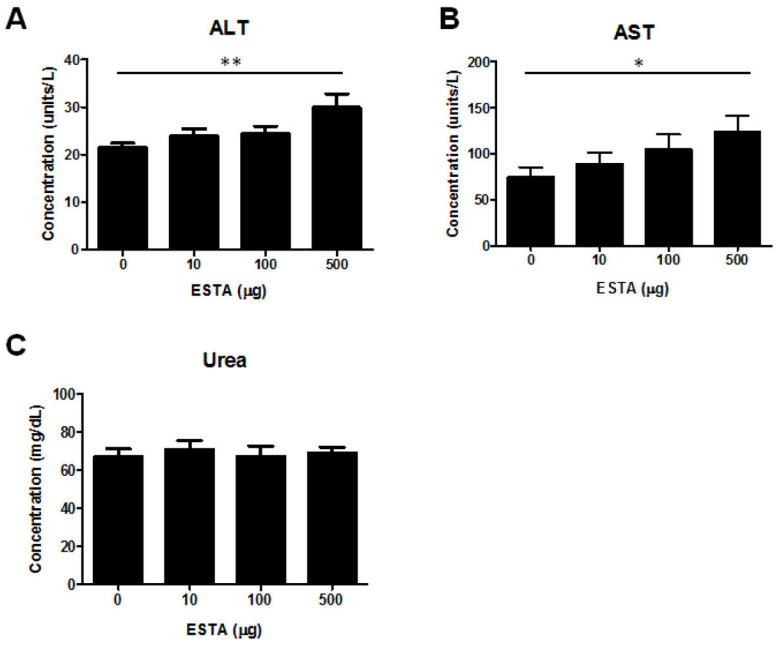

Figure 1.

Levels of plasma ALT (A), AST (B), and urea (C) in mice that were administered 10, 100, or 500 μg of ESTA intravenously, twice a week for 4 weeks. The plasma was isolated from whole blood collected 2 days after the last injection. The data represent Mean ± *SEM* (n=7–9). Statistical significance was determined by linear regression models (*, p<0.05; **, p<0.01).

A

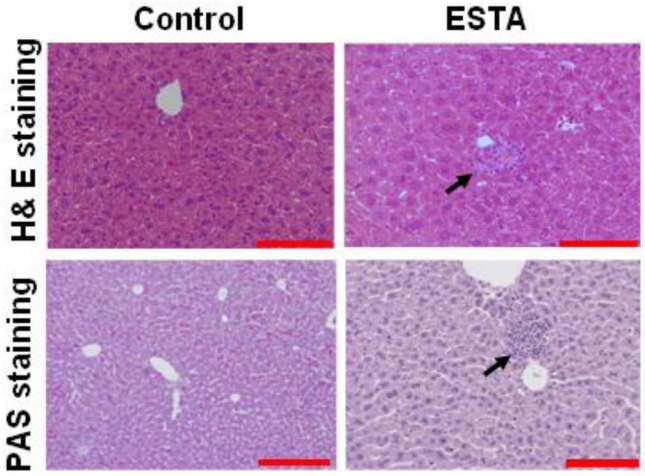

B

	Number of necrotic foci	Necrotic foci poitive mice (%)	Sum of necrotic area / total area (μm2)
Saline	0	33.3	18603
ESTA (500μg)	1.5 **	75	2825

Figure 2.

Effect of repeated intravenous administrations of ESTA on hepatic toxicity. The livers from mice that received repeated intravenous injections of ESTA were harvested 2 days after the final injection and fixed with formalin. Paraffin sections were stained with H&E or PAS for histological analysis. (A) The H&E-stained lung tissue of the mice injected with saline or 500 μg of ESTA in a repeat-dose subacute study. (B) The PAS-stained liver from the mice injected with 500 μg of ESTA in a repeat-dose subacute study. The black arrow indicates the microscopic foci. The images were captured at a final magnification of 200×. The scale bars represent 100 μm.

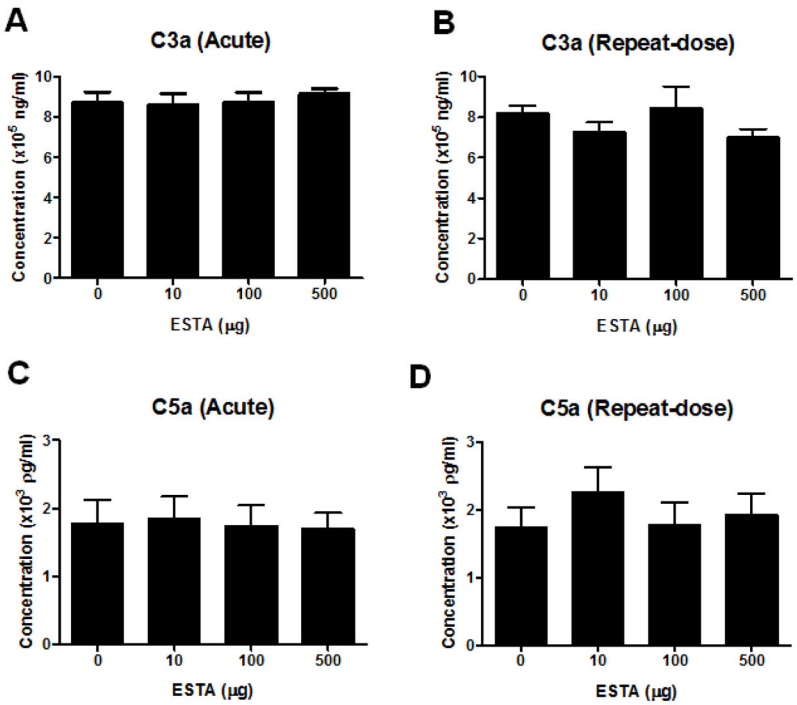

Figure 3.

Effect of single or repeated intravenous administration of 10, 100, or 500 μg of ESTA on complement C3a and C5a plasma concentrations. Plasma concentrations of complement factors 3a (A and B) and 5a (C and D) were measured from samples collected 4 hours after a single intravenous injection of ESTA (A and C) or 2 days after the last injection of a repeat-dose subacute study (B and D). The data represent Mean ± *SEM* (*n*=7–9).

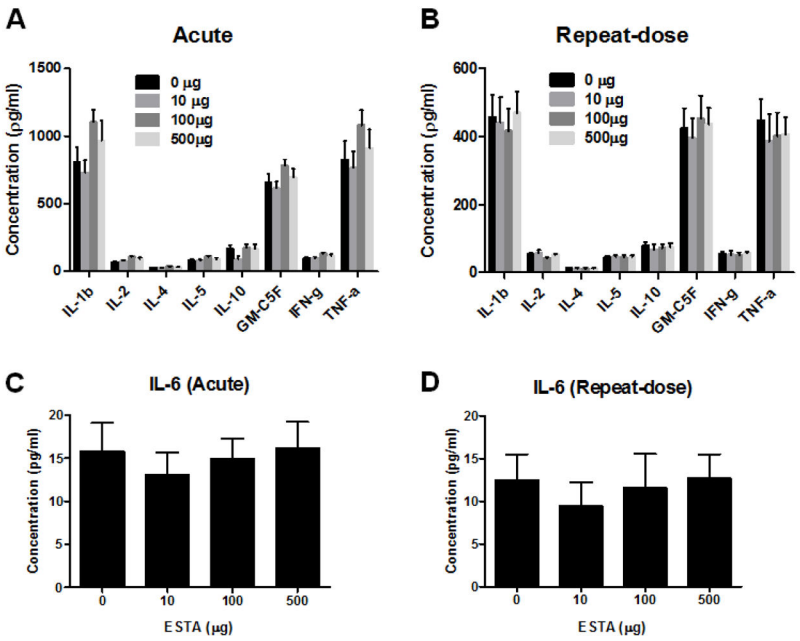

Figure 4.

Effect of single or repeated intravenous administration of 10, 100, or 500 μg of ESTA on plasma levels of cytokines. Plasma concentrations of eight different cytokines (IL-1β, IL-2, IL-4, IL-5, IL-10, GM-CSF, IFN-γ, and TNF-α; A and B) and IL-6 (C and D) were measured from samples collected 4 hours after a single intravenous injection of ESTA (A and C), or 2 days after the last injection of a repeat-dose study (B and D). The data represent Mean ± *SEM* (*n*=7–9).

Table 1

Hematological analysis of whole blood samples following a single intravenous administration of ESTA.

Parameters	Unit	ESTA (μg)			
		0	10	100	500
RBC	$\times 10^6$ cells/μl	9.0±0.2	9.1±0.3	9.1±0.3	8.9±0.3
WBC	$\times 10^3$ cells/μl	4.9±0.5	5.0±0.6	5.3±0.6	5.8±0.4
Lymphocytes	%	64.6±1.3	67.4±1.4	66.8±2.8	60.6±2.1
Monocytes	%	5.3±0.7	5.5±0.5	5.7±0.6	5.4±0.7
Neutrophils	%	29.5±1.6	26.2±1.1	27.0±2.8	33.5±2.1
Eosinophils	%	0.6±0.3	0.9±0.2	0.5±0.3	0.6±0.2
Basophils	%	0.1±0.4	0±0	0±0	0±0

Values represent mean ± *SEM*

Table 2

Hematological analysis of whole blood samples following repeated intravenous administration of ESTA.

Parameters	Unit	ESTA (μg)			
		0	10	100	500
RBC	$\times 10^6$ cells/μl	8.7±0.3	8.6±0.2	8.4±0.2	8.7±0.2
WBC	$\times 10^3$ cells/μl	7.11±0.4	8.0±0.5	7.7±1.1	8.8±0.8
Lymphocytes	%	73.3±1.2	73.0±0.9	70.4±2.0	70.3±2.4
Monocytes	%	4.2±0.2	3.9±0.1	4.0±0.1	3.8±0.2
Neutrophils	%	22.5±1.3	23.1±1.0	25.6±2.0	25.9±2.4
Eosinophils	%	0±0	0±0	0±0	0±0
Basophils	%	0±0	0±0	0±0	0±0

Values represent mean ± *SEM*